

Supporting Information

Morphology-Patterned Anisotropic Wetting Surface for Fluid Control and Gas-Liquid

Separation in Microfluidics

Shuli Wang,[†] Nianzuo Yu,[†] Tieqiang Wang,[‡] Peng Ge,[†] Shunsheng Ye,[†] Peihong Xue,[†]
Wendong Liu,[†] Huaizhong Shen,[†] Junhu Zhang^{*,†}, and Bai Yang[†]

[†]State Key Laboratory of Supramolecular Structure and Materials, College of Chemistry, Jilin University, Changchun 130012, P. R. China

E-mail: zjh@jlu.edu.cn

[‡]Research Center for Molecular Science and Engineering, Northeastern University, Shenyang 110004, P. R. China

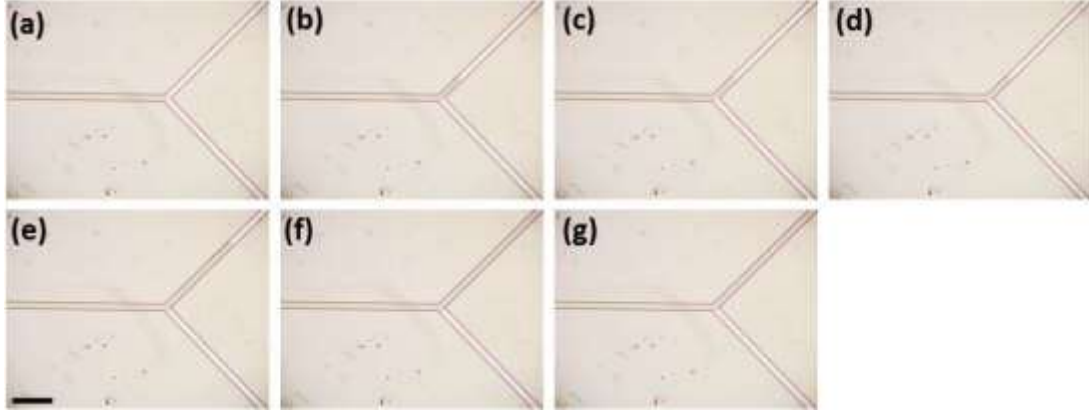


Figure S1. Detailed flow behavior of water in Y-shaped microchannel on PFS-modified patterned surface with Si stripes (Microchannel: top = 146 μm , bottom = 200 μm , height = 25 μm ; Applied pressure: 45 mbar). The scale bar is 1 mm.

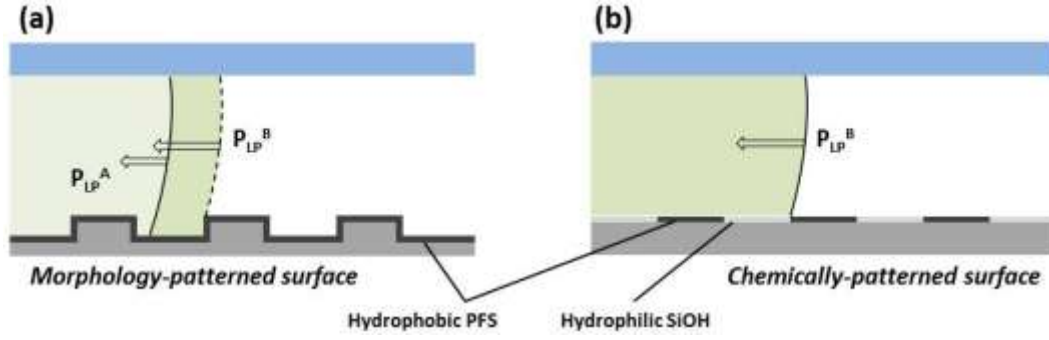


Figure S2. The mechanism of the occurrence of energy barrier in microchannels built on (a) morphology-patterned surface and (b) chemically-patterned surface.

Explanation of the mechanisms

The unidirectional/anisotropic flow behavior of water in the microchannel on morphology/chemically patterned surface could be ascribed to the energy barrier that exists in the perpendicular direction. In two kinds of microchannel, the reason for energy barrier is different. As shown in the schematic illustration below, the energy barrier is originated from the Laplace pressure (P_{LP}) on morphology patterns or chemical patterns. In microchannels, Laplace pressure strongly affects the microfluid, which is governed by surface wettability and channel size as represented by the Young-Laplace equation:

$$P_{LP} = -2\gamma/R = -2\gamma \cos\theta/r \quad (1)$$

where γ is surface tension, R is radius of liquid curvature, θ is surface contact angle and r is channel radius. When the surface is hydrophobic ($\theta > 90^\circ$), P_{LP} takes a positive value and thus work as a pressure barrier upon introduction of water. As a result, introduction of water into the channel requires increasement of hydraulic pressure to overcome P_{LP} (P_{LP}^A in Figure S2). In microchannel built upon physically-patterned surface, when the front surface of the water reaches the entrance of the narrower channel (Figure S2(a)), water stops at the boundary due to the larger P_{LP}^B in the narrower channel. To introduce water into the narrower channel, hydraulic pressure higher than P_{LP}^B is required. Thus, in microchannel on physically-patterned surface, pressure barrier is originated from periodic structural change in the size.

But in microchannel built upon chemically patterned surface, a change in the surface wettability can induce pressure barrier (shown in Figure S2(b)). When water crosses the hydrophilic SiOH area and arrives at the boundary of hydrophilic-hydrophobic stripes, increasement of hydraulic pressure is required due to the pressure barrier induced from P_{LP}^B . So in microchannel on chemically-patterned surface, pressure barrier is originated from PFS area of periodic hydrophilic-hydrophobic stripes. Therefore, for physically and chemically-patterned surface, the reason of Laplace pressure that induces pressure barrier is different. In microchannel on physical patterns, water showed unidirectional flow behavior under a driving pressure of 50 mbar, and gas-water interface at the junction was stable, and no water flow was found in outlet perpendicular to the stripes. However, in microchannel on chemically-patterned surface, water showed anisotropic flow behavior and it flowed in the outlet perpendicular to the stripes, although the flow speed was much lower than it in the another outlet. According to the above results, we could conclude that the movement of three phase contact line in the perpendicular direction is difficult on physically-patterned surface compared to chemically one.

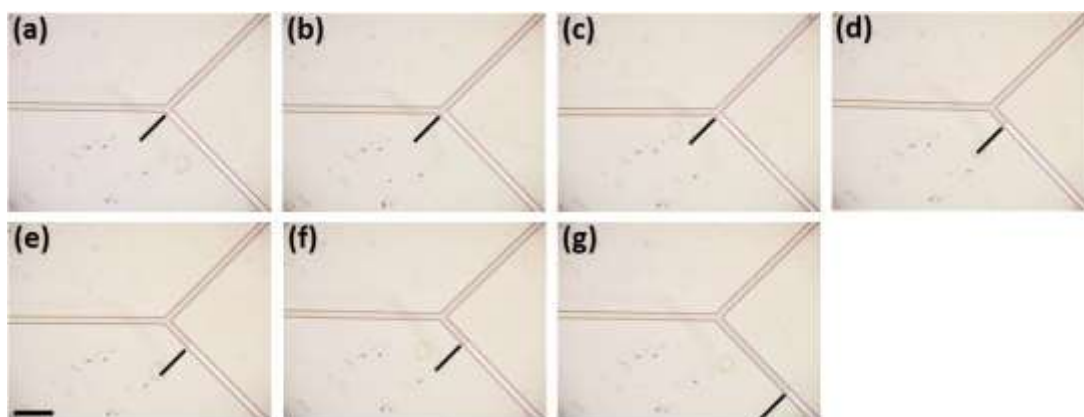


Figure S3. Optical microscopy images of water flowing distance in Y-shaped microchannel on PFS-modified Si stripes at different driving pressure. The pressure in image (a-g) is 40, 45, 50, 55, 60, 70, 80 mbar, respectively. The black lines represent the flowing distance of water in outlet 2. The scale bar is 1 mm.

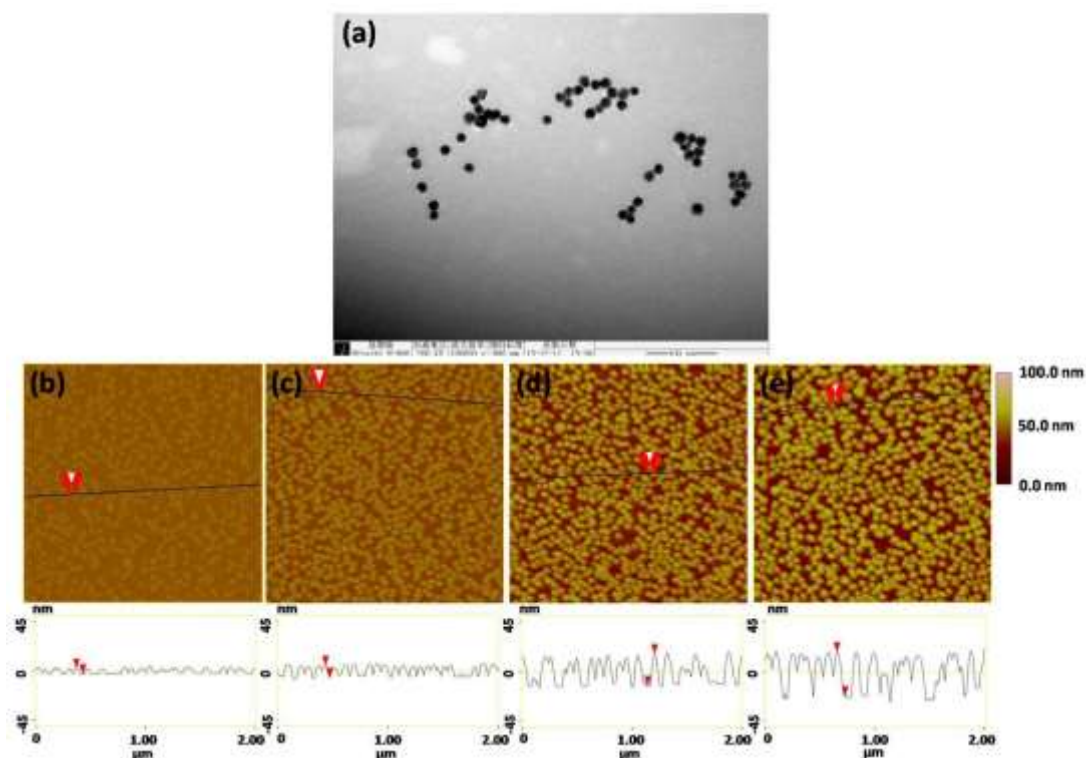


Figure S4. (a) TEM image of the synthesized Au NPs. (b-e) AFM images of the nanoscale structures of different roughness. The etching duration of RIE process is 10, 20, 30, and 45 s, respectively. The underlying profiles show the height of the obtained nano structures after RIE process.

Table S1 The relationship between etching duration, height of the nano structures and roughness of the stripes.

Etching time [s]	Height [nm]	Roughness [nm]
10	4.741±0.353	1.670
20	11.082±0.572	4.145
30	28.097±1.247	8.928
45	38.600±3.894	12.400

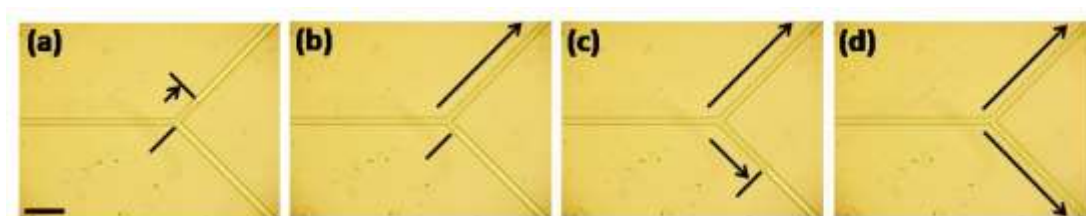


Figure S5. The flowing process of water in microchannel built on the APTES-modified Si stripes. The applied pressure is 45 mbar. The scale bar is 1 mm.

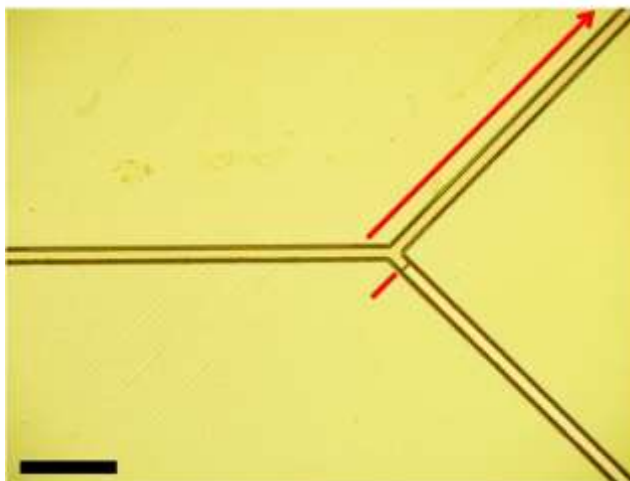


Figure S6. In microchannel with the height of 63.5 μm (the width is 200 μm), water does not show unidirectional flow even at a low driving pressure (30 mbar). The scale bar is 1 mm.

Table S2 Surface tension values of solution of different mass fraction of ethanol, and their detailed flowing parameters in microchannel upon Si stripes. The stripes are 20 μm in period, and 600 nm in depth. The driving pressure is 50 mbar.

wt%	Surface tension [mN m ⁻¹]	D2 [mm]	D2/D1
0.0	71.93	0.00	0.000
2.0	64.61	0.10±0.03	0.020
5.0	56.47	0.11±0.02	0.022
10.0	49.49	0.64±0.06	0.128
15.0	43.22	1.61±0.23	0.322
20.0	40.04	3.85±0.50	0.770

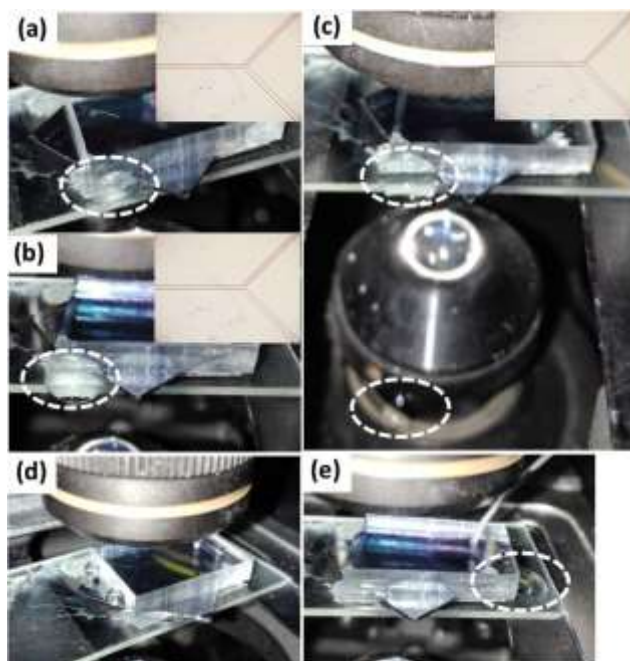


Figure S7. (a-c) The stability of gas-water interface formed in the beginning of outlet 2 when water was injected continuously for 30 min. It remained its initial position even if water flowed through outlet 1 and accumulated to a big droplet and dropped down from the glass slide under the microdevice. The leakage pressure of the microdevice: (d) no water leakage between two plates at an applied pressure of 150 mbar, (e) water leakage occurred when the applied pressure was 200 mbar. Inside the white dashed lines are water droplets.

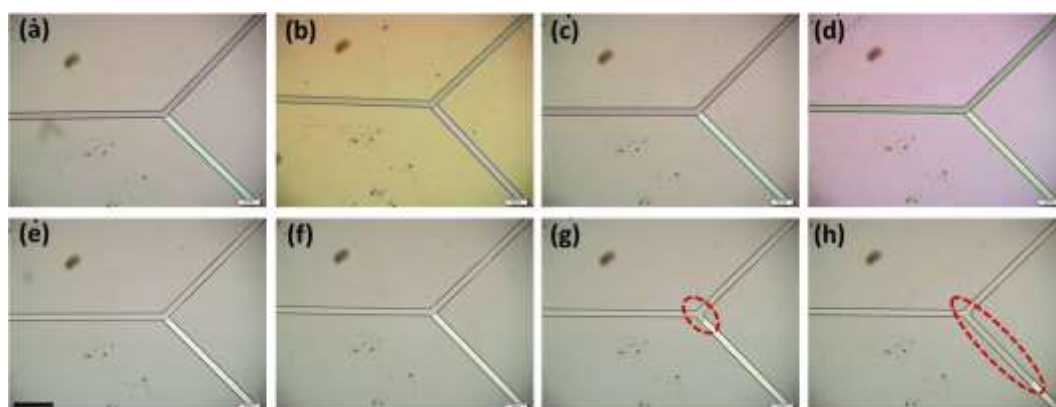


Figure S8. Comparison of the stability between the physical and chemical patterns. (a-d) and (e-h) are water flow behavior in microchannels on morphology- and chemically- patterned surfaces of SiOH-PFS stripes, respectively. The surfaces in image (a) and (e) were untreated, and the others were treated in different condition: (b) and (f) were thermally treated at the temperature of 60 °C for 4 hour; (c) and (g) were covered by PDMS sheet for 4 hour; (d) and (h) were covered by PDMS sheet at the temperature of 60 °C for 4 hour. In image (g) and (h), water flowed 0.14 ± 0.06 and 2.19 ± 0.64 mm in the perpendicular direction, respectively, when it flowed 3.44 mm in the parallel direction. Thus, the surface property of the chemically-patterned surface changed when covered by PDMS sheet (especially in a high temperature condition), while the property of physically-patterned surface remained unchanged, indicating the stability of physical patterns are better than chemical patterns. The scale bar is 1 mm.

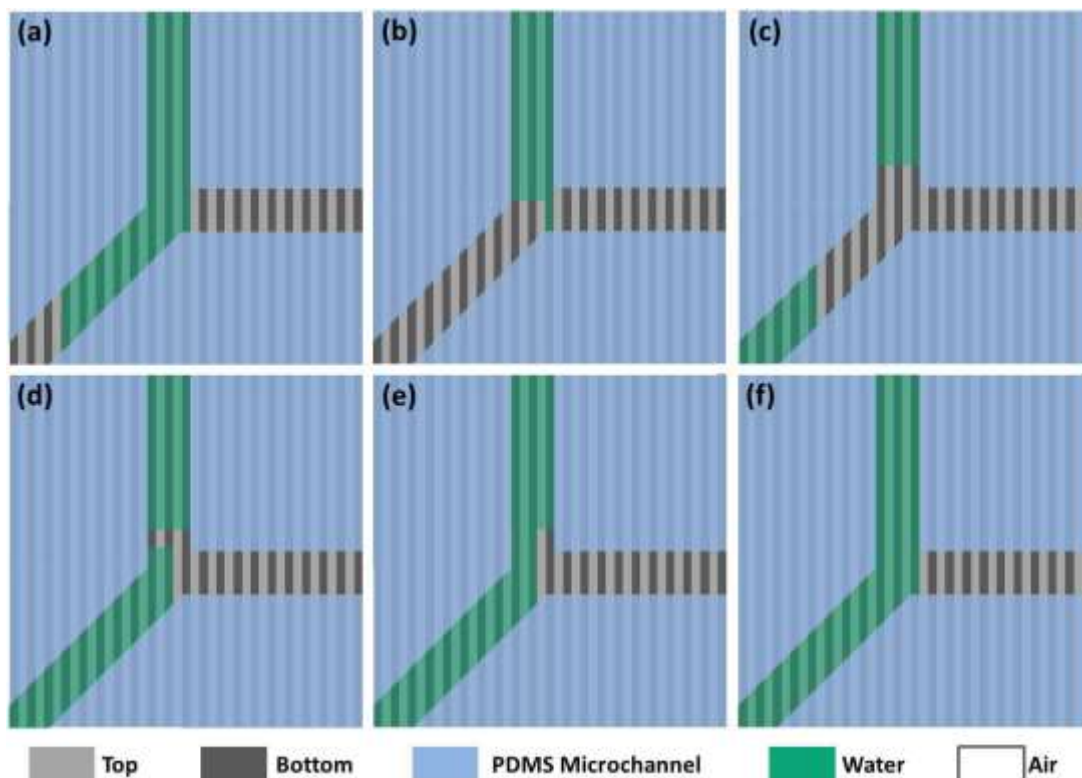


Figure S9. Schematic illustration of gas-water separation process in microchannel upon morphology-patterned surfaces. (a) When water arrived at the Y-junction, it was directed to outlet 1 due to anisotropic wetting of patterned surface. (b-c) When air plugs reached the junction, it pushed water to a small distance until it broke the gas-water interface in the beginning of outlet 2. Once the gas-water interface was broken, air plugs entered and then flowed away from outlet 2, because the hydrodynamic resistance for the flow of air plug in outlet 1 was significantly higher than that in outlet 2. (d-e) The position of water in outlet 1 remained unchanged until the next water slugs arrived to the junction. (f) Although a small part of air exist in outlet 1, it was pushed to outlet 2 when water arrives the junction, as a result, water and air flowed into outlet 1 and 2, respectively.

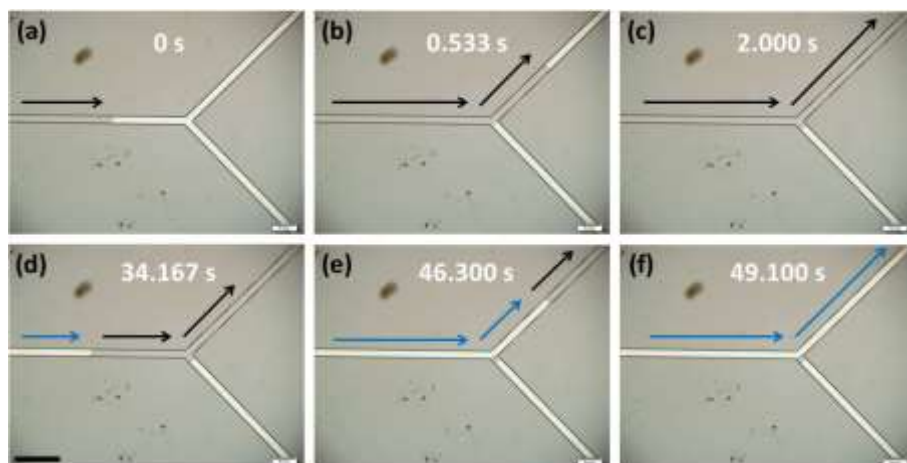


Figure S10. Failure of gas-water separation in microchannel built upon chemcially-patterned surface of SiOH-PFS stripes. (a-c) Water flowed anisotropically in the separating channel, and a small water plug occured in the outlet 2. (d-f) When the air slug arrived the junction, it also flowed through outlet 1, because the hydrodynamic resistance in outlet 1 was lower than that in outlet 2. The small water plug in outlet 2 provided a big resistance for the flow of air in outlet 2. Because water and air plug both flowed through the outlet 1, the separation of gas and water mixture was failed. The black arrows represent the flow direction of water and the blue arrows represent the flow direction of air. The scale bar is 1 mm and driving pressure is 47 mbar.